SECOND EUROPEAN CONFERENCE ON EARTHQUAKE ENGINEERING
AND SEISMOLOGY, ISTANBUL AUG. 25-29, 2014

RESPONSE REDUCTION OF BASE ISOLATED STRUCTURES BY INERTIAL MASS DAMPERS

Koichi SUGIMOTO[1] , Akira FUKUKITA[2] and Yoshihisa KITAMURA[3]

ABSTRACT

A rotating inertial mass damper consists of a ball screw mechanism including a flywheel. This damper has been proven to have significant mass damping effects because of the ball screw mechanism, even if the mass of the flywheel is small.

This paper presents the effect of response reduction by rotating inertial mass damper and spring in series applied to a seismic isolation system. We conducted a shaking table test of a single-degree-of-freedom (SDOF) model composed of a weight and four coil springs with a damper and spring in series when the series spring was fixed and operated. The stiffness of the series spring was determined about 1.5 times as large as the stiffness of the main system spring by theoretical calculation in order to reduce the acceleration response of the base isolated structure. When the spring was fixed, the displacement and acceleration of the seismic isolation layer was able to be reduced by the damper against the long-period earthquake motions. In the short-period earthquake motions, the displacement of the seismic isolation layer was reduced, but the acceleration of the seismic isolation layer was increased by increasing inertial mass. On the other hands, increase of the acceleration of the seismic isolation layer was suppressed by operating the series spring in the case of the short-period earthquake motions.

We also conducted a dynamic loading test of a rotating inertial mass damper with an actuator, in order to clarify the inertial mass and damping force which the damper can hold. Based on these data obtained from the shaking table test and dynamic loading test, we constructed a numerical analysis model, in order to simulate the shaking table tests. The results of numerical analysis showed very good agreement with the results of shaking table test.

INTRODUCTION

Rotating inertial mass dampers were developed as a vibration control device and have begun to be applied to actual buildings in recent years. Inertial mass dampers generate inertial force of thousands of times of their mass weight, by utilizing the inertial mass effect determined by the outer diameter of the flywheel and the rotating ball screw lead. The damper then reduces response that would be caused by having the inertial force act on the structure.

In this paper, we report on the effect of reduction of the response by the inertial mass damper and spring in series when applied to base isolated structure, obtained from the results of numerical analysis and shaking table tests. In order to investigate the effect of the response reduction of the base isolated structure by the the inertial mass damper and spring in series, we conducted a shaking table test, where the parameters were inertial mass and earthquake motions. We also conducted a dynamic

[1] Research Engineer, Shimizu Corporation, Tokyo, k_sugimoto@shimz.co.jp
[2] Senior Research Engineer, Shimizu Corporation, Tokyo, fukukita@shimz.co.jp
[3] Deputy General Manager, Shimizu Corporation, Tokyo, kitamura@shimz.co.jp

loading test of the rotating inertial mass damper with an actuator and clarified the inertial mass and damping force, which the damper can hold by itself. Then we constructed a numerical analysis model and verified the validity of this model by comparing the analytical results with the experimental results. We investigated the relationship between the characteristic of the input ground motion and reduction of response by the inertial mass damper and spring in series conducting the shaking table test and numerical analysis.

OVERVIEW OF THE SHAKING TABLE TEST

Inertial mass dampers were developed as a vibration control device and have begun to be applied to actual buildings in recent years. An inertial mass damper consists of a ball screw mechanism including a flywheel. This damper has been proved to have significant mass damping effects because of the ball screw mechanism, even if the mass of the flywheel is small.

We show a photo and the specifications of inertial mass damper in Figure 1 and Table 1. This inertial mass damper has a removable structure with 0 to 3 pieces of flywheels in one ball screw. So that inertial mass ψ shown in Equation (1) can be changed in four steps 0.3 and 2.1, 3.9, 5.7 tons.

$$\psi = \frac{\pi^2 D^2}{2L_d{}^2} m \tag{1}$$

Here, D is the diameter of the flywheel, L_d represents the lead of the ball screw, m is the mass of the flywheel. The damper has an inertial mass of 0.3 tons by rotating the ball nut and ball screw and so on, even if the flywheel is not attached. The stroke of this damper is ± 350mm , and the total length of the damper is about 1100mm.

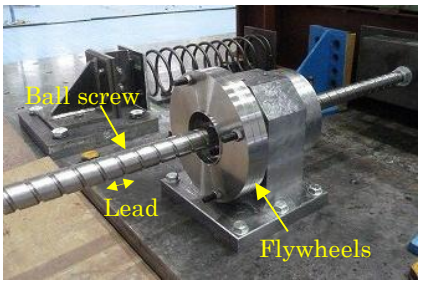

Figure 1. Photo of an inertial mass damper

Table 1. Specifications of an inertial mass damper

Inertial mass(tons)	0.3, 2.1, 3.9, 5.7
Maximum capability of axial force(kN)	40
Ball screw lead L_d(mm)	40

The layout of the specimen is as shown in Figure 2. The specimen is a vibration system of single-degree-of-freedom (SDOF) that consists of four coil springs and a weight. The inertial mass damper and one spring were connected in series to the weight. The weight moves on a pair of a linear guide, so it can move only in one direction. We measured the acceleration of the weight and shaking table, and the displacement of the weight, the damper and the spring in series. Figure 3 shows the photo of the specimen. Figure 4 shows the transfer function of the acceleration response of the weight and the shaking table. The transfer function is shown in the case of vibrating the specimen which has no inertial mass damper and without series spring under the white noise. From this result, we identified the natural frequency and the damping factor of the specimen and these values were shown in Table 2.

As shown in Table 2, the stiffness of the series spring was determined 30(N/mm) by theoretical calculation in order to reduce the acceleration response of the base isolated structure. We show below

a method to determine the stiffness of series spring. Figure 5 shows the acceleration response spectrum of the earthquake motions in the case of El Centro wave and Sannomaru wave, respectively. Figure 6 shows the response ratio of acceleration in the case of connecting the inertial mass damper and spring in series to this SDOF specimen. When the inertial mass of the damper was 2.1 ton, the stiffness of series spring was changed from 30(N/mm) to 900(N/mm) in four steps. From Figures 5 and 6, when the stiffness of series spring is large (equivalent to the case of without series spring) the maximum value of the response ratio is high and overlaps with predominant frequency of short-period earthquake motion such as El Centro wave. On the other hand, when the stiffness of series spring is small, the maximum value of the response acceleration is shifted to the long-period side and response ratio tends to decrease. The acceleration of the weight was reduced effectively to use the soft spring. As described above, we decided to connect a soft spring in series to the inertial mass damper of 30 (N/mm) in order to suppress the response acceleration of the weight.

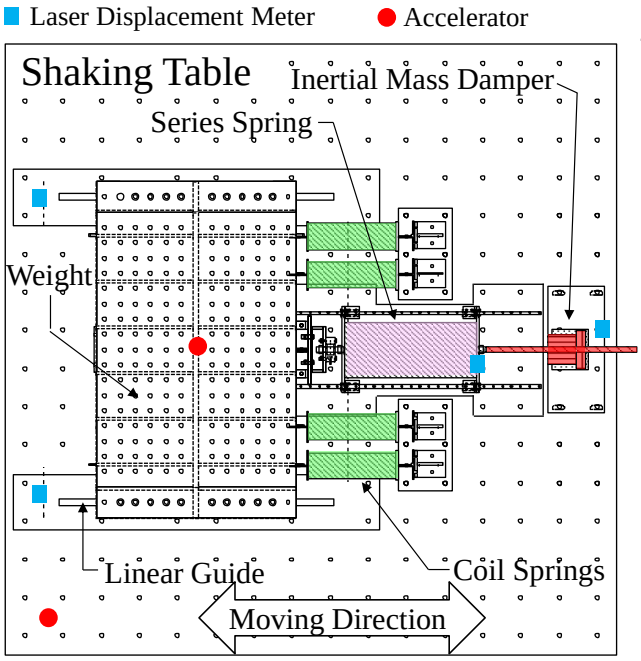

Figure 2. Layout of specimen

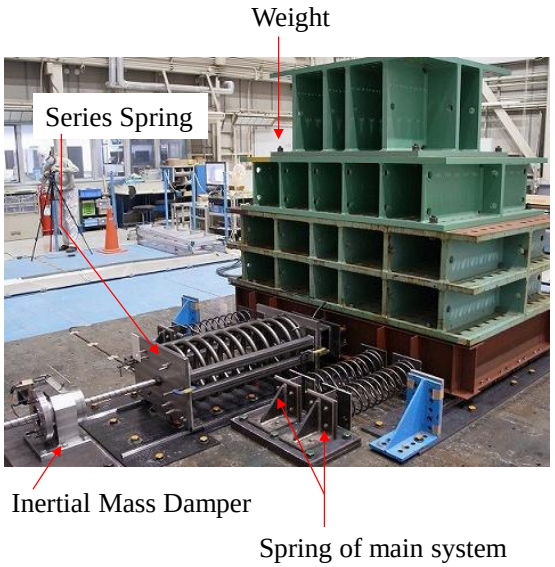

Figure 3. Photo of the specimen

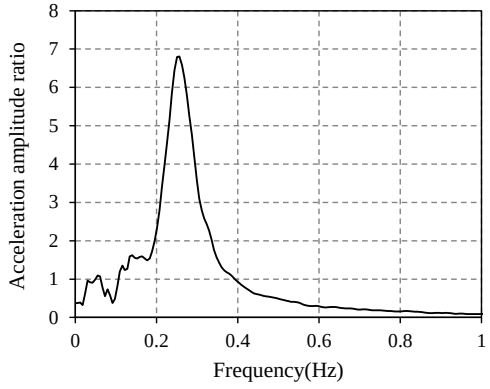

Figure 4. Transfer function of the specimen

Table 2. Specification of specimen

Weight(ton)	7.6
Natural frequency(Hz)	0.25
Damping factor	0.11
Stiffness of the series spring(N/mm)	30

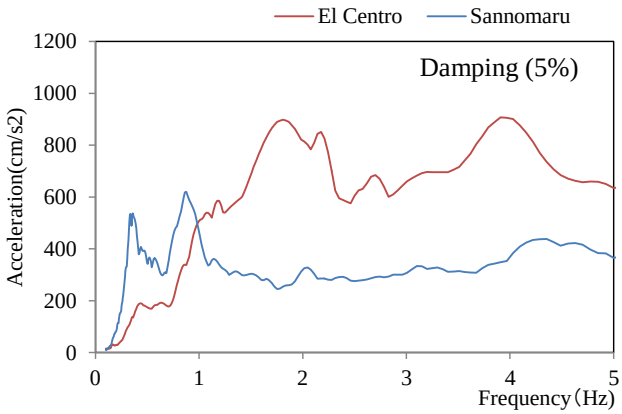

Figure 5. Acceleration response spectrum of earthquake motions

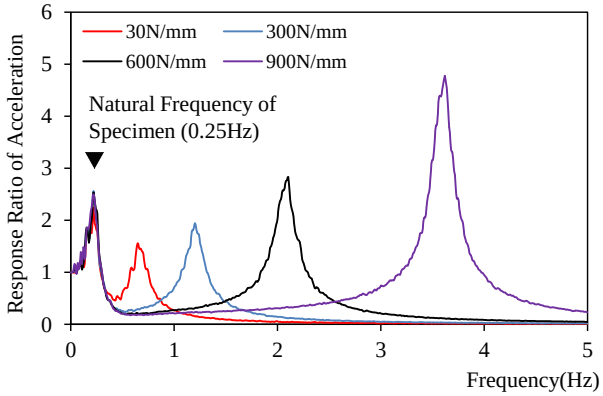

Figure 6. Acceleration response ratio of the specimen in the case of changing series spring stiffness

In order to verify the response reduction by the inertial mass damper and spring in series, we vibrated the shaking table using earthquake motions with different characteristics. Table 3 shows the input earthquake motions that were used in the shaking table test. El Centro wave and Sannomaru wave were selected as representative of the short-period and long-period earthquake motions, respectively. The input acceleration amplitude of the earthquake motions was scaled in order that the displacement of the specimen was about 300mm without the inertial mass damper and spring in series.

Table 3. Earthquake motions

case	Maximum acceleration(cm/s^2)
El Centro NS	758
Sannomaru	202

TEST RESULT

Figure 7 shows the maximum response displacement and response acceleration of the weight when the series spring was fixed or operated using the El Centro wave and Sannomaru wave. According to Figure 7, when the spring was fixed, the acceleration and displacement of the weight was able to be reduced by the damper against the long-period earthquake motions such as Sannomaru wave. In the short-period earthquake motions such as El Centro wave, the displacement of the weight was able to be reduced, but the acceleration of the weight was increased by increasing inertial mass of the damper. On the other hands, increase of the acceleration of the weight was able to be suppressed by operating the series spring in the case of El Centro wave, and the response of acceleration in the case of Sannomaru wave was not increased by operating the series spring. Figure 8 shows the displacement ratio and acceleration ratio of the maximum response value of the operated series spring to fixed series spring. In the case of operated series spring, acceleration of the weight was reduced about 45% compared to that of fixed series spring, and displacement of the weight was increased by 10% when the inertial mass was 2 ton shown in Figure 8 (a) El Centro. When the inertial mass is in the range of up to 4 tons in the case of Sannomaru wave shown in Figure 8 (b), the response of acceleration was not increased by operating the series spring, so we confirmed the reduction of response by the inertial mass damper and the spring in series. When inertial mass ratio of the weight (7.6ton) is large, inertial mass is 4 ton or more, the response of the weght is increased.

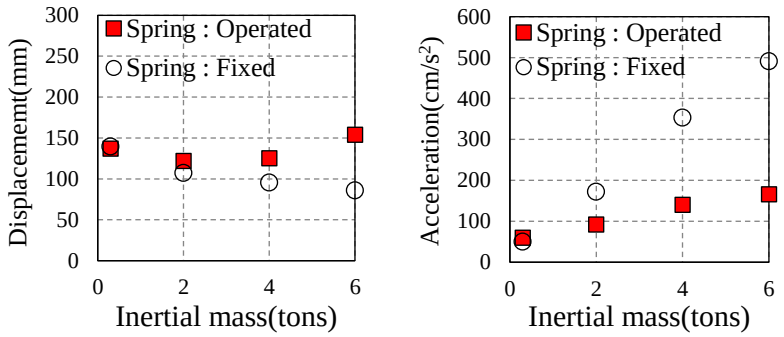

(a) El Centro wave

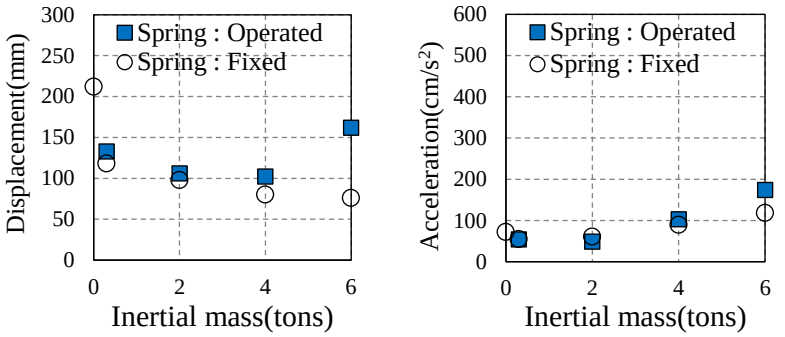

(b) Sannomaru wave

Figure 7. Relationship of the maximum reseponse value and inertial mass

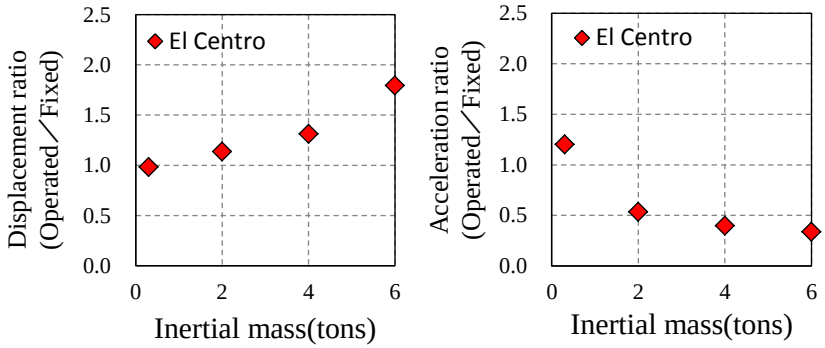

(a) El Centro wave

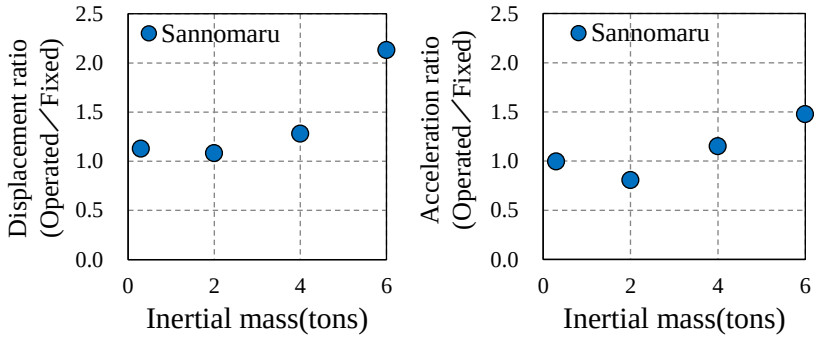

(b) Sannomaru wave

Figure 8. Relationship of the maximum reseponse value and inertial mass

SIMULATION ANALYSIS

First, we describe the construction of the analysis model to be used in the numerical analysis. A numerical analysis model of the single degree of freedom system simulated specimen of the shaking table test is shown in Figure 9. Here, k_1, c_1 shows the stiffness and damping coefficient of seismic isolation layer, ψ shows the inertial mass, c_2 shows the damping coefficient of the inertial mass damper. And k_2 shows the stiffness of a spring connected in series with the inertial mass damper. The damping coefficient c_1 of the isolation layer was calculated using a transfer function of the specimen shown in Figure 4 and damping factor of the specimen is 0.11.

We conducted a dynamic loading test of a rotating inertial mass damper with an actuator and measured the axial load of the damper by load cell and displacement of the damper. The experimental set up to measure the axial load and displacement of the damper is shown in Figure 10. At that time, we vibrated the damper by changing the inertial mass and the frequency of the sine wave. Frequency of the sine wave was varied from 0.25Hz to 1.0Hz, and the displacement amplitude of vibration was $\pm$ 10mm. As an example, Figure 11 shows the load-displacement relationship when we vibrated the damper attached to 2 flywheels at 0.25Hz sine wave. From this loop, we calculated damping coefficient of the damper by the Equation (2). Here, ΔW is the total area of the loop, ω is the circular frequency, and $\delta_{\max}$ is the maximum displacement of the damper. As a result of the calculation using the Equation (2), the damping coefficient of the loop in Figure 11 is 10.3×10^{-3}(kNsec/mm). Table 4 shows the damping coefficients calculated from the all vibration cases. From Table 4, the damping coefficient of the damper is varied by inertial mass and frequency of the sine wave. The range of the damping coefficients is from 4.5×10^{-3} to 10.3×10^{-3}(kNsec/mm). Figure 12 shows the relationship of the maximum force and relative velocity of the damper for every inertial mass. The relative velocity

was calculated from frequency of the sine wave and the maximum displacement of the damper. In this paper, from Figure 12, we apply 4.0×10^{-3}(kNsec/mm) to the value of c_2, it is average value of the damping coefficient calculated from the slope of each inertial mass.

$$c_2 = \frac{\Delta W}{\pi\omega\delta^2{}_{\max}} \tag{2}$$

When the velocity is high area, the c_1 and c_2 become small compared with the case of low velocity area. So c_1 and c_2 were modeled with the skeleton of a non-linear against relative velocity of the damper, as shown in Figure 13. The specification about the skeleton of c_1 and c_2 are shown in Table 5. Here, α is the reduction ratio of the damping coefficient when the velocity of the damper is 20 (cm/s) or more. Specifications of the analysis model used in this paper are shown in Table 6.

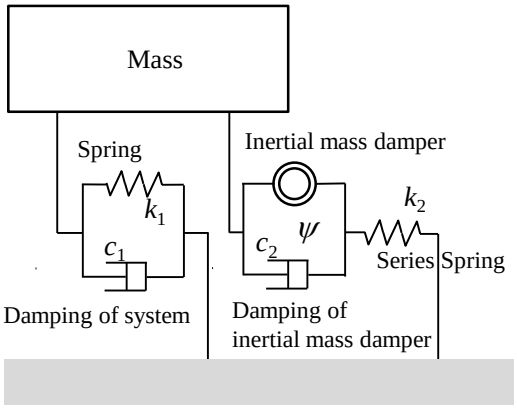

Figure 9. Analysis model

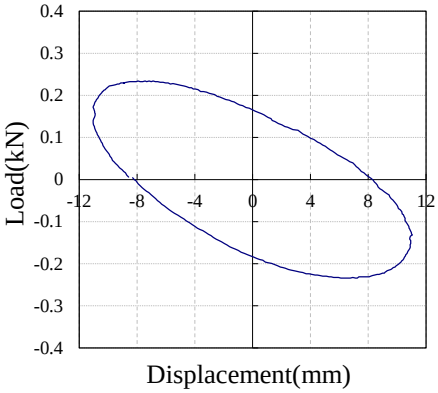

Figure 11. Load-displacement relationship (0.25Hz, Inertial mass:3.9ton, c_2:4.0*10^{-3}(kNsec/mm))

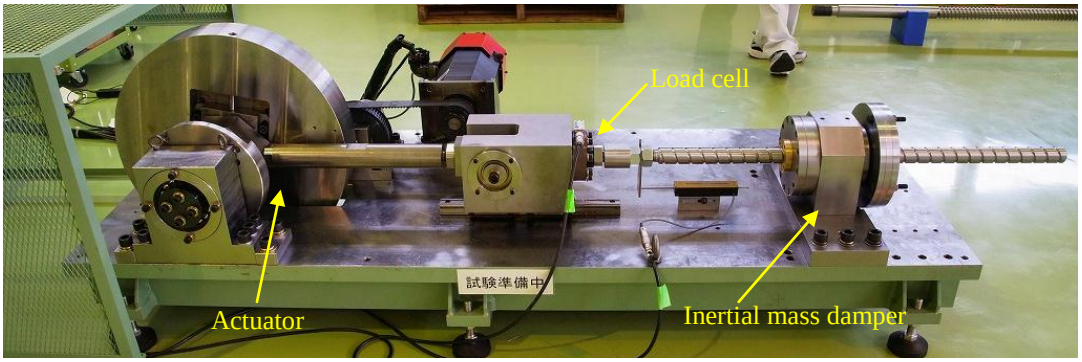

Figure 10. Experimental set up to measure the axial load and displacement

Table 4. Damping coefficient of inertial mass damper

		Inertial mass (ton)			
		0.3	2.1	3.9	5.7
Frequency of the sine wave(Hz)	1.00	5.5	5.7	4.5	6.1
	0.75	4.8	4.7	5.4	4.6
	0.5	6.4	6.8	6.5	6.5
	0.3	8.3	8.9	8.4	6.8
	0.25	8.8	9.0	10.3	9.0

unit : $\times10^{-3}$kNsec/mm

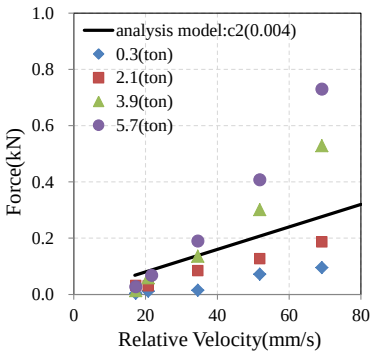

Figure 12. Relationship of maximum force and relative velocity of the damper

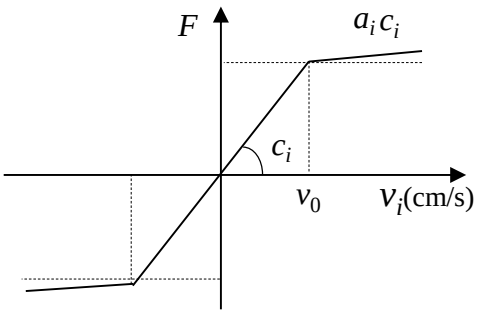

Figure 13. Skeleton of the damping elements

Table 5. Specifications of damping coefficients

	c_i(kNs/mm)	v_0(cm/s)	α_i
c_1	2.7*10^{-3}	20.0	0.075
c_2	4.0*10^{-3}	20.0	0.270

Table 6. Specifications of analysis model

Mass M (ton)	7.6
Natural frequency (Hz)	0.25
Stiffness of series spring (N/mm)	30.0
Inertial mass (tons)	2.1

We compared experimental results and analytical results for the time history waveform of the acceleration response and displacement response in the case of El Centro wave and Sannomaru wave. The results of these comparison are shown in Figures 14 and 15. From these Figures, the maximum amplitude value and the phase of the displacement waveform and acceleration waveform are shown to be almost identical in the analytical results and the experimental results.

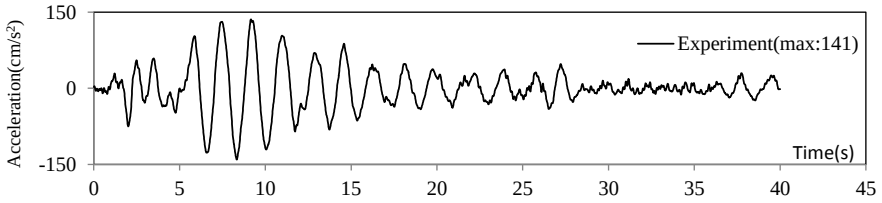

(a) Acceleration waveform (experiment)

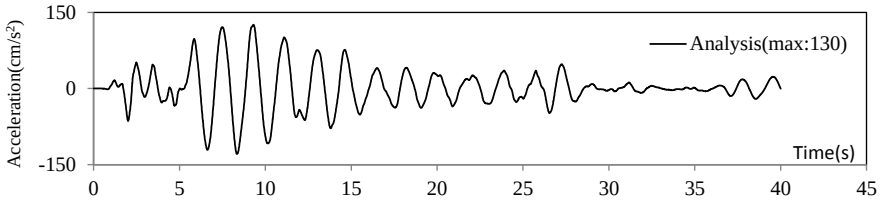

(b) Acceleration waveform (analysis)

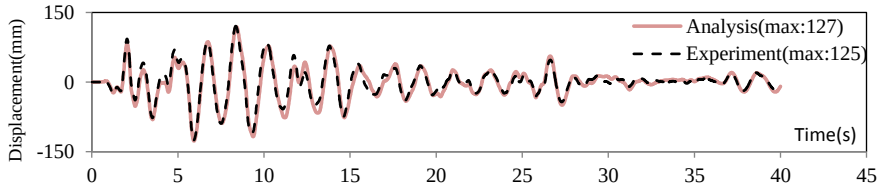

(c) Displacement waveform (experiment and analysis)

Figure 14. Verification of the analysis model (El Centro)

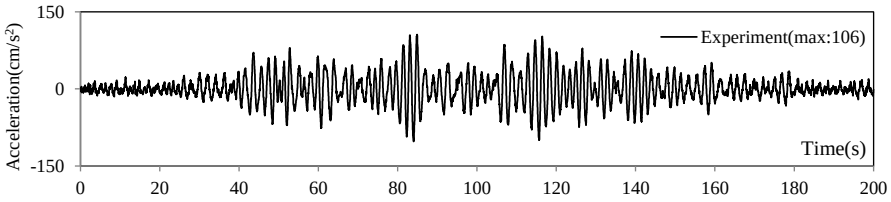

(a) Acceleration waveform (experiment)

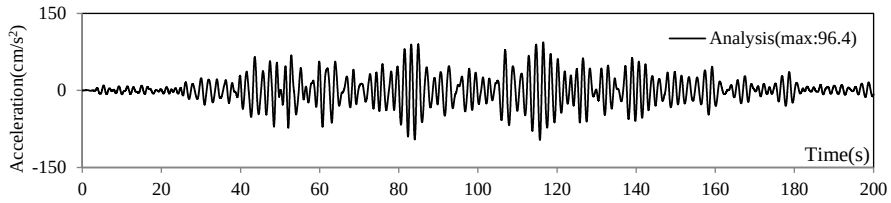

(b) Acceleration waveform (analysis)

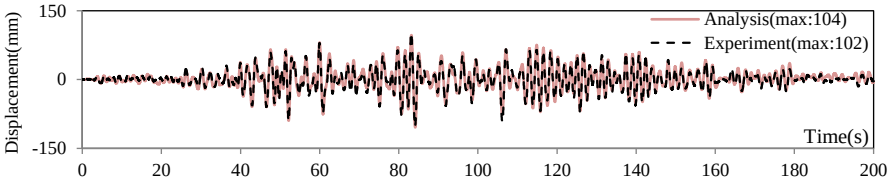

(c) Displacement waveform (experiment and analysis)

Figure 15. Verification of the analysis model (Sannomaru)

CONCLUSIONS

We verified the reduction of response relative to the input ground motions with different characteristics by conducting a shaking table test of a SDOF model with the inertial mass damper and spring in series on a base isolated structure. As a result, when the spring was fixed, the damper was able to reduce the acceleration and displacement of the weight against the long-period earthquake motions such as Sannomaru wave. In the short-period earthquake motions such as El Centro wave, the displacement of the weight was reduced, but the acceleration of the weight was increased by increasing inertial mass. On the other hands, increase of the acceleration of the weight was suppressed by operating the series spring in the case of El Centro wave. Acceleration of the weight operated series spring was reduced about 45% compared to that of fixed series spring, and displacement of the weight increase by 10% in the case of 2 ton of inertial mass. Moreover, we constructed an analysis model of an SDOF system that simulates the shaking table test and we verified the validity of the model by comparing the analytical results with the experimental results. At that time, damping of main system and inertial mass damper was found to be non-linearly against the velocity.

Future, we are planning to conduct the analysis using an analysis model of inertial mass damper constructed in this paper, and develop a seismic isolation system that is more effective response reduction.

REFERENCES

Isoda, K., Hanzawa, T. and Tamura, K. : A study on response characteristics of a SDOF model with rotating inertia mass dampers. *Journal of Structural and Construction Engineering*, AIJ, Vol.74 No.642, 1469-1476, Aug., 2009.

Nakaminami, S., Kida, H., Ikago, K. and Inoue, N.: Application of viscous mass damper with force restriction mechanism to base-isolated structures and its effectiveness. *Journal of Structural and Construction Engineering*, AIJ, Vol.76 No.670, 2077-2086, Dec., 2011.

Hanzawa, T., Isoda, K. : Vibration Control By A TMD Using A Rotating Inertial Mass, *Proceedings of the 15th World Conference on Earthquake Engineering*, Lisbon, 2012, Paper No. 3342.